Effect of Air Flow Rate Variation on the Performance of an Indirect Solar Dryer Using Flat and Perforated Absorber Plates

Ghadeer Qasim Fadhil [iD] [✉]*, **Sarmad A. Abdul Hussein** [iD] [✉]

Department of Mechanical Engineering, College of Engineering, University of Baghdad, Baghdad, Iraq

ABSTRACT

An experimental analysis was conducted to investigate the effect of varying the inlet airflow rate into the drying chamber on the performance of an indirect solar dryer using a forced convection system under the climatic conditions of Baghdad, Iraq, at a latitude of 33.3°N. The dryer performance was tested at three airflow rates (0.0113, 0.0169, and 0.0226) m^3/s, using a conventional flat absorber plate and a perforated plate with circular holes of diameter 3 mm. Apricots were dried in all experiments conducted in June 2024. The results showed that the perforated plate significantly enhanced the thermal efficiency of the solar collector compared with that of the flat plate. The perforated plate improved the heat exchange by disturbing the thermal boundary layer and improving airflow. The results also indicated that a low airflow rate (0.0113 m^3/s) achieved the best drying efficiency, reducing the apricot moisture content from 80% to 42% for the perforated plate and 47% for the flat plate within 8 h, with maximum drying efficiencies of 28.44% and 22.22%, respectively. Although a higher airflow rate (0.0226 m^3/s) improved the thermal efficiency of the collector, it was less effective for enhancing the drying process. The results of this study demonstrated that operating an indirect solar dryer with a perforated absorbent plate at a low airflow rate accelerates the removal of moisture from the product while maintaining its quality. This makes the system suitable for practical agricultural applications in hot and dry environments, where drying speed and efficiency are critical for reducing postharvest losses and increasing product storage life.

Keywords: Air flow rate, Collector thermal efficiency, Dryer efficiency, Forced convection, Indirect solar air dryer.

1. INTRODUCTION

Agricultural products are essential export commodities for numerous countries globally. Nonetheless, their moisture level presents a considerable rotting risk during storage and transportation **(Srithanyakorn et al., 2023)**. Drying is one of the first operations farmers

perform in the chain of processing steps to extend the storage duration of agricultural products **(Ndukwu et al., 2023)**. Utilizing fossil fuels for drying incurs significant costs and environmental concerns. A sustainable solution to this problem can be provided by using solar energy for drying, a renewable energy source. Solar drying is one of the most efficient and environmentally friendly technologies **(Ennissioui et al., 2023)**. Sun drying is a traditional way to dry agricultural products. This method is practiced in many developing countries since the energy necessary for this process is free, renewable, non-polluting, and abundant in most environments. Sun drying depends on weather conditions, as the product is exposed to solar radiation, dust, and insects, resulting in low-quality products. The products dried using traditional methods are unacceptable in the market, which is an economic loss for the country **(Khan et al., 2018)**. Indirect solar drying constitutes a significant preservation methodology for vegetables and fruits **(Lingayat et al., 2020)**. Indirect solar drying offers a higher level of control over the drying process and results in products of superior quality compared to sun drying due to the absence of direct exposure of the products to solar radiation during the drying phase. Thus, they are shielded from the adverse impacts of ultraviolet radiation. The drying occurs indirectly through convection between warm air and the products designated for drying **(Krabch et al., 2022)**. **(Farhan and Sahi, 2017)** designed and manufactured three solar air heaters with two perforated plates and one smooth absorber plate. The best exit air properties were obtained using a perforated absorber plate. **(Al-Juamily et al., 2007)** investigated experimentally the feasibility of utilizing collectors as air heating devices in product drying systems. The trials were conducted at the Energy and Environment Research Center, which falls under Baghdad's Ministry of Industry and Minerals. The results found that the primary variable affecting the drying rate is the air temperature entering the cabinet.

(Jassim and Shbailat, 2018) evaluated five varieties of solar collectors: traditional channel with a flat absorber plate (sample I), double channel with a flat absorber plate (sample II), double channel with perforating "V" corrugated absorber plate (sample III), double channel with internal connected wire mesh (sample IV), and double channel with absorber sheet of transparent honeycomb, (sample V). The best results were employing the sample (III) compared with other cases. **(Nhut et al., 2020)** conducted a set of experiments with crimped baffles to obtain a suitable outlet air temperature from the solar collector for an agricultural dryer in Bienhoa City, Vietnam. **(Essalhi et al., 2017)** designed an indirect solar dryer with natural convection for the dehydration of pears. At the commencement of the drying process, the initial mass of the pears was recorded as 997.3 g, experiencing a substantial decrease, culminating in a final weight of 135.13 g after 24 hours of drying. The mean drying chamber thermal efficiency was 11.11%. **(Hegde et al., 2015)** designed and studied an indirect active solar dryer, evaluating the efficacy of a smooth absorber plate solar collector in two configurations, top flow and bottom flow, for the dehydration of banana slices. Their results indicated that the bottom flow design produced chamber temperatures about 2.5°C higher than those obtained with the top flow configuration. Furthermore, the bottom flow configuration demonstrated a 38.21% enhancement in efficiency compared to the top flow configuration, which demonstrated an efficiency of 27.5%.

(Bhavsar and Patel, 2021) developed and constructed a solar air dryer utilizing natural and forced convection air drying techniques in the Ahmedabad region of India. The study aimed to assess the efficacy of the solar dryer. The collector's efficiency was recorded at 19.27% in natural convection mode and 35.60% in forced convection mode. The solar air dryer with forced convection mode effectively dried products with high moisture content.

(Nabnean and Nimnuan, 2020) designed a direct solar air dryer under forced convection for drying bananas. Its performance was compared with conventional sun drying. The results demonstrated that the dry air temperature within the dryer fluctuated between 35 °C and 60 °C from 8:00 A.M. to 6:00 P.M. Moreover, the direct solar dryer with forced convection reduced the moisture content of bananas 48% more rapidly than sun drying. **(El-Sebaey, 2024)** developed an indirect solar dryer incorporating a fan (forced convection) and a chimney (natural convection) to assess their impact on drying efficiency and evaporation rate for grape drying in Egypt. Results indicated that the moisture content of the grape sample for the chimney declined from 79.80% to 14.04%, while the moisture content for the fan declined to 15.83% throughout three days of experimentation. **(Zeeshan et al., 2024)** designed an indirect forced convection solar dryer and performance evaluation at the Solar Energy Research Lab, NUST Pakistan. Tomatoes were dried as the experimental product. Results indicate that the dryer's efficiency was 50.14% on day one, 66% on day two, and an overall efficiency of 58.07%. **(Arunkumar et al., 2024)** developed an indirect solar dryer by incorporating glass fragments and paraffin wax as natural materials to retain heat energy inside the solar collector. They evaluated its performance in reducing the moisture content of red pepper. Results found that the indirect solar dryer used with glass fragments and paraffin wax demonstrated sustained drying durations and improved product quality. **(Rezaei et al., 2022)** studied the influence of sewing machine pulley metal and PCM (phase change material) on the absorber plate inside a solar collector on the dryer's performance. The results indicated that implementing the absorption plate with a sewing machine pulley and PCM enhances the average efficiency of the solar collector and the dryer.

(Mugi et al., 2022) investigated an analysis of energy and exergy by using indirect natural and forced convection solar dryers, comparing the results. The transient temperature and humidity distribution within the dryer trays, along with the collector and drying chamber energy efficiency metrics, were evaluated for both types of dryers. The energy and exergy analysis indicated that the performance efficacy of the indirect solar dryer with forced convection surpassed that of natural convection. A solar dryer prototype incorporating a photovoltaic system and electrical resistance was created and evaluated by **(Salhi et al., 2024)**. The experiments in August 2023 were taken in eastern Morocco (the mechanical and energy laboratory). The new prototype's overall efficiency was evaluated by drying the sample of tomatoes. The consequences displayed that the efficiency of the drying of the dryer ranges from 60% to 100% during the day. **(Natarajan et al., 2024)** executed an experimental investigation to evaluate the efficacy of forced and natural convective drying techniques in comparison with the conventional open-sun drying method. Tested how well each technique reduced the grapes' moisture content. The results demonstrated that forced convection reduced the moisture content of grapes by an astounding 83.21%, whereas open-sun drying reduced it by 30.5% over three days. On the other hand, natural convection removed 82.35% of the moisture, while open-sun drying removed 25.05%. **(Babar et al., 2020)** designed and manufactured the passive solar air dryer with a smooth absorber plate collector for drying agricultural products. Mushrooms were dried in the passive dryer and compared to sunlight drying. The samples' moisture ratio was zero after 21 hours of drying in a passive solar dryer and 33 hours in the sunlight drying. The solar air dryer passive took 36.36% less period than sunlight drying. The solar dryer passive can dry samples in 35–40% less period than the sunlight drying. **(Jadallah et al., 2020)** investigated an experimental study of a mixed-mode solar air dryer with forced convection with a dual counter-flow photovoltaic-thermal hybrid system for drying agricultural products. The system's

performance was evaluated by drying banana slices, proving the ability to dry in large percentages. **(Kumar et al., 2022)** formulated a mathematical model derived from the experimental data to assess the design parameters of an indirect solar dryer under both no-load and full-load conditions. The study concluded that the efficiency of the drying of the solar dryer was enhanced by fan-assisted forced convection. **(Kokate et al., 2023)** assessed the efficacy of an indirect solar air dryer by comparing it with conventional solar drying for dehydrating onion and garlic products. They found that indirect solar drying technology was more effective in drying products than conventional solar drying. **(Gilago and Chandramohan, 2022)** performed an experimental study to evaluate the effectiveness of forced and natural convection indirect-type solar dryers in the dehydration of ivy gourd. **(Fernandes et al., 2022)** created and evaluated two prototypes from indirect solar dryers for drying vegetables and fruits. The result indicated the feasibility of drying items to less than 10% of their original weight at a low cost. **(Vijayan et al., 2020)** developed and studied an indirect forced convection solar dryer with a porous layer as a thermal storage medium under the climatic conditions of Coimbatore for drying bitter gourd slices. The study aimed to investigate the impact of air mass flow rate on the efficiency of a solar drying system. **(Tagne et al., 2022)** performed a study that evaluated the efficacy of a solar dryer developed explicitly for drying cocoa beans. The dehydration procedure utilized natural convection overnight and forced convection during the day.

Based on the review above, there has been a growing interest in developing and enhancing indirect solar air dryers for diverse crops. Despite this increasing interest, many existing studies have not adequately addressed the performance of such systems under the specific environmental and climatic conditions in Iraq. Therefore, this study aims to improve the efficiency of an indirect solar air dryer system by studying the effect of changing airflow rates (0.0113, 0.0169, and 0.0226) m^3/s entering the drying chamber. In addition, a comparison is made between the thermal performance of a conventional flat absorber plate and a perforated absorber plate with circular holes of diameter 3 mm inside a solar air collector. Apricots were chosen as the drying material. The study included measuring temperatures, solar collector efficiency, drying efficiency, drying rate, and moisture content at three different airflow velocities. The experiments were conducted under Iraqi weather conditions to better understand the impact of the local climate on the overall system performance.

## 2. EXPERIMENTAL APPARATUS AND PROCEDURE

An indirect solar dryer under forced convection was designed and fabricated to dry vegetables and fruits. The dryer is made of economically viable and environmentally sustainable materials. The experimental apparatus comprised two fundamental elements: a solar air collector and a drying chamber. **Fig. 1** represents the experimental apparatus schematically, and **Fig. 2** photographically.

2.1. Solar Air Collector

The major component of a solar dryer is a solar collector, consisting of an absorber plate that helps heat the air and a glass cover, which induces the greenhouse effect. The air trapped between the glass cover and absorber plate gains maximum heat from solar radiation and then transfers to the product placed in the drying chamber **(Ennissioui et al., 2023)**, as shown in **Figs. 3a** and **3b**. The solar air collector is designed with dimensions of 100 cm in

length, 80 cm in width, and 20 cm in height, and the structural frame is made of 18 mm thick wood to prevent heat loss. The solar air collector was inclined at an angle of 30°. Two types of absorption plates were manufactured from aluminium metal with dimensions of 80 cm in length, 80 cm in width, and 1 mm thick. The first plate was a conventional flat plate, and the second plate was perforated with circular holes on its surface with a diameter of 3 mm, as shown in **Fig. 4**.
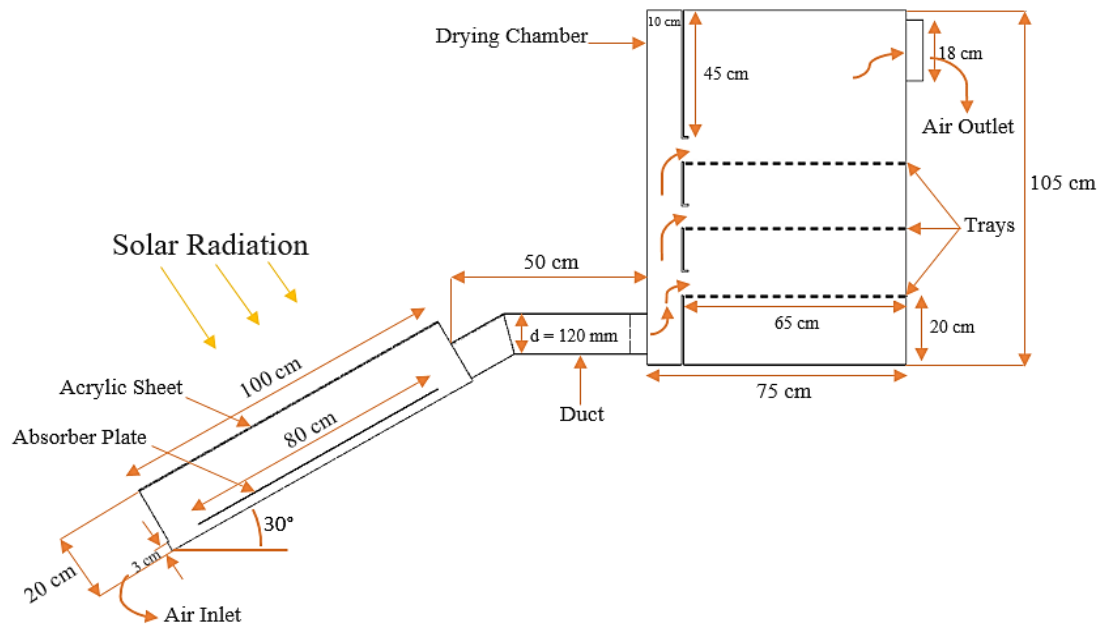
Figure 1. Schematic diagram of the experimental apparatus.
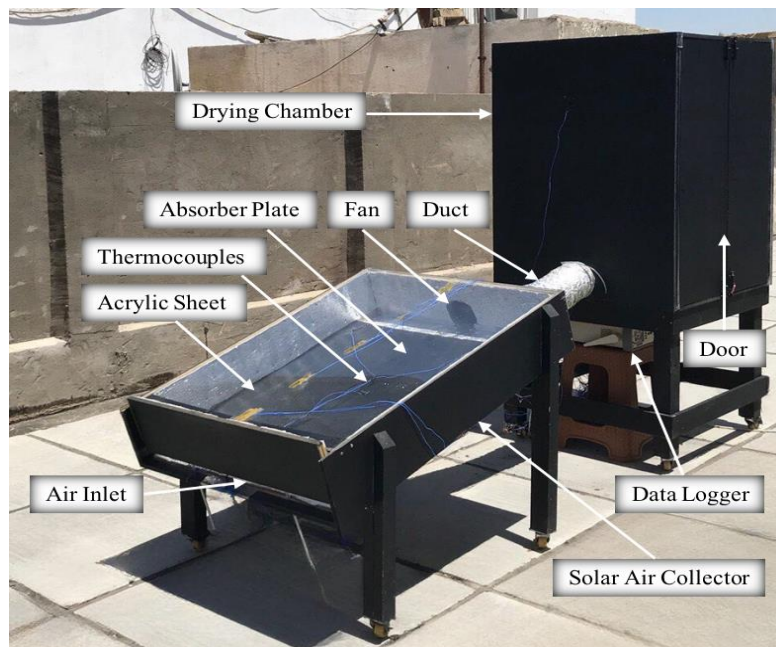
Figure 2. Photograph of the experimental apparatus.

The absorption plates were painted with matte black paint to enhance heat absorption. The solar collector roof structure is covered with acrylic sheet dimensions 100 cm in length, 80

cm in width, and 4 mm thick. The gap of 17 cm between the absorption plate and the acrylic sheet facilitates air circulation. The solar collector is insulated on all sides with a 10 mm thick layer of polyethylene foam to reduce heat losses. To draw outside air through the solar collector inlet into the drying chamber, an axial fan with a diameter of 120 mm was placed at the collector outlet. The air duct is constructed from aluminium with a length of 50 cm and a diameter of 120 mm. It is insulated with a layer of glass wool through which the hot air is transferred from the solar collector to the drying room without any heat loss.

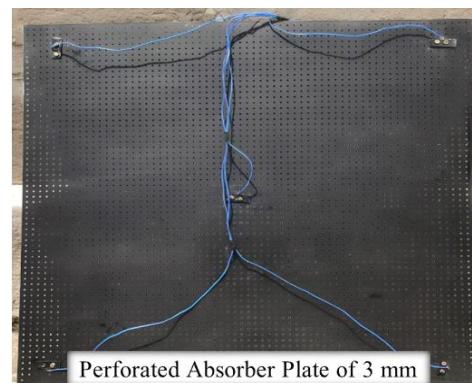(a)   (b)

Figure 3. (a) and (b) Solar air collector.
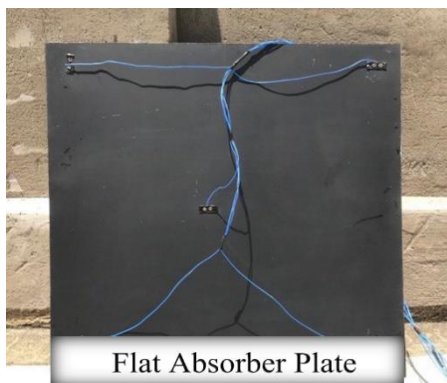
(a)   (b)

Figure 4. Type of the absorber plates.

2.2. Drying Chamber

The drying chamber was designed with dimensions of 75 cm in length, 75 cm in width, and 105 cm in height. The frame was made of 18 mm thick wood. All sides were insulated from the inside with a layer of 10 mm thick polyethylene foam to reduce heat loss. Three trays made of aluminium mesh were placed with dimensions of (65 x 75) cm, and a distance of 20 cm was left between each tray. The vertical air distribution channel is integrally designed inside the drying chamber to facilitate uniform hot air distribution to each tray. The modern

air distribution mechanism has improved the dryer effectiveness and quality of dried products in the solar drying system **(Sileshi et al., 2022)**, as shown in **Fig. 5a**. The dryer door was constructed from wood with dimensions of (75 × 100) cm. Hot air rises between the trays and leaves through a circular opening with a 180 mm diameter located at the top end at the back of the drying chamber to control airflow through the dryer, as shown in **Fig. 5b**.

(a)   (b)
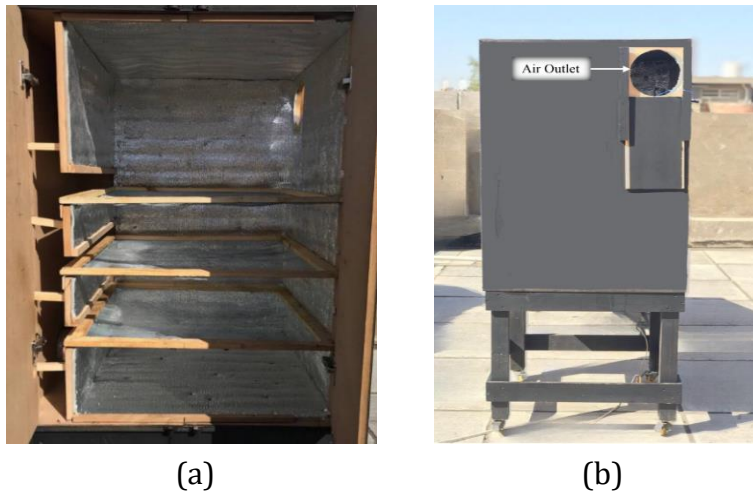
Figure 5. (a) Drying chamber. (b) Air outlet.

2.3. Experimental Procedure

Experiments were carried out under Baghdad's city's local weather conditions to assess the effectiveness of the indirect forced convection solar air dryer. The experiments were conducted in June 2024. The experimental testing was initiated at 8:00 AM and concluded at 16:00 PM. The data was recorded on an hourly basis. The essential parameters monitored during the experimental work were the inlet and outlet air temperatures of the collector, the temperature of the absorber plate, air temperature on the trays, air relative humidity, solar radiation, and dried sample weight. The experimental tests were at three airflow rates (0.0113, 0.0169, and 0.0226) m^3/s. The airflow rate is regulated by controlling the fan speed with a fan controller at the outlet of the solar collector. The temperature points are measured by the type - k thermocouples with an uncertainty of ± 0.1°C. These thermocouples are interfaced with a temperature data logger (AT4532x) and accommodate a 32-channel. The weight of the dried samples was determined throughout the drying period using a precise digital weighing scale with an accuracy of ±0.1 g and a capacity of 10,000 g. The airflow velocity at the entrance of the dryer was measured by a digital data-logging hot wire anemometer (YK-2005AH). The relative humidity was measured by Environment Meter EM-9000 with a range between 0 to 95% R.H. with an accuracy of ± 3% and a resolution of 0.1%. Hourly solar radiation data were taken from the Ministry of Science and Technology/Renewable Energy Department for Baghdad city, where the latitude coordinate is 33.3° north. Approximately 3 kg of apricots were used to assess the system's efficacy in dehydrating agricultural products. The quantity of apricots was about 80% relative humidity. The product was washed off with clean water, and the cores were removed. The product was allowed to dry before being evenly distributed across three trays, and its weight was measured before the drying process. The loss of humidity was estimated by determining the weight loss.

3. THERMAL ANALYSIS

Experimental calculations assessed the operational efficacy of the solar air dryer. The air mass flow rate (ṁ) directed towards the dryer is calculated by multiplying the air density (ρ), the cross-sectional area of the airflow channel (A_{duct}), and air velocity (v), as shown in Eq. (1), **(Al-Neama, 2018)**:

$$\dot{m} = \rho \, A_{duct} \, v \tag{1}$$

Where v is the air velocity (m/s), and A_{duct} is the area of the airflow channel is calculated as:

$$A_{duct} = \frac{\pi}{4} \, d_{duct}^{\,2}$$

The useful heat energy (Q_u) of the solar air collector was obtained from Eq. (2);

$$Q_u = \dot{m} \, Cp \, (T_o - T_i) \tag{2}$$

Where C_p is specific heat (J/kg °C), T_i is the solar collector inlet temperature, and T_o is the solar collector outlet temperature.

The input thermal solar radiation (Q_{solar}) into the collector can be calculated by Eq. (3);

$$Q_{solar} = I \, Ac \tag{3}$$

Where I is the total value of incident solar radiation intensity (W/m^2), and Ac is the area of a solar collector (m^2).

The thermal efficiency (η_c) for a solar air collector can be calculated by Eq. (4);

$$\eta_c = \frac{Q_u}{Q_{solar}} \tag{4}$$

The moisture content of the product decreases during the drying process. The moisture content percentage (MC) can be calculated by Eq. (5), **(Ssemwanga et al., 2020)**:

$$MC(\%) = \frac{m_i - m_f}{m_i} *100\% \tag{5}$$

Where m_i and m_f represent the sample's mass before drying and after drying, respectively.

The mass of the evaporated water (m_w) can be calculated by Eq. (6), **(Kilanko et al., 2019)**:

$$m_w = \frac{m_i \, (M_I - M_F)}{100 - M_F} \tag{6}$$

Where M_I represents the initial moisture content, and M_F represents the final moisture content.

The drying rate (m_{dr}) can be calculated by Eq. (7), **(Kilanko et al., 2019)**:

$$m_{dr} = \frac{m_w}{t_d} \tag{7}$$

Where t_d is the overall drying time.

The solar dryer efficiency $\left(\eta_d\right)$ is calculated by Eq. (8) **(Khidhir, 2023)**:

$$\eta_d = \frac{m_w \; h_{fg}}{I \, A_c \; t_d} \tag{8}$$

Where h_{fg} represents the latent heat vaporization for water from steam tables = 2270 kJ/kg at an average temperature.

4. RESULTS AND DISCUSSION

The experimental results are presented and analyzed to study the impact of changing the airflow rate on the solar air dryer's performance using the perforated absorber plate with circular holes with a diameter of 3 mm and compared with a flat absorber plate.

Fig. 6 shows the variation in solar radiation intensity from 09:00 AM to 16:00 PM in June 2024. The solar radiation intensity rises in the early morning, peaks at 13:00 PM with a maximum value of 821.62 W/m², and then decreases and disappears at sunset. The figure indicates that the intensity of solar radiation varies based on the weather conditions on the respective days when the readings were recorded. The variation in solar radiation intensity of the curves is a slight difference of ± 1 to 25 W/m². Although this difference was slight, its impact on the system's thermal performance was minimal, demonstrating its ability to operate efficiently under natural solar radiation variations, confirming its practical suitability for agricultural applications in hot climates.
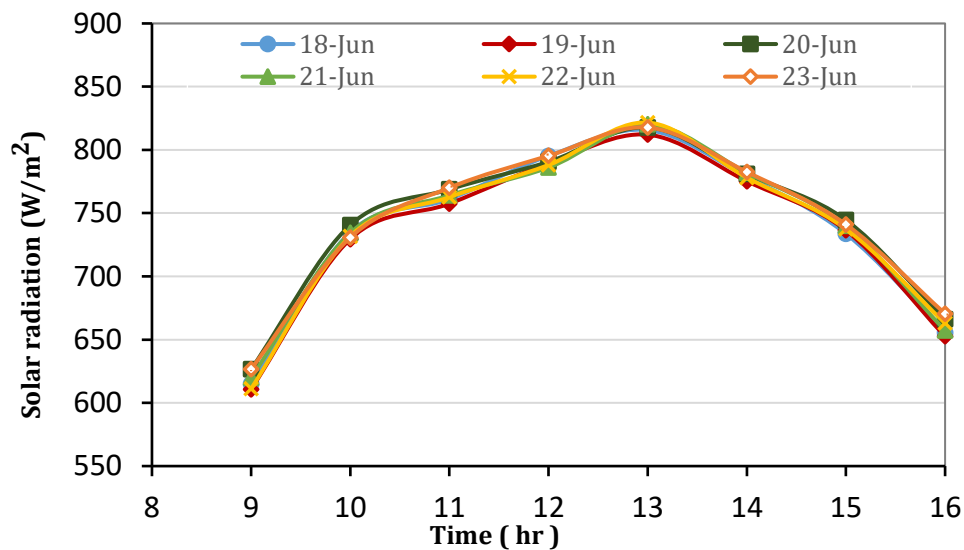

Figure 6. Variation of solar radiation intensity with local time

Fig. 7 shows the average temperature of the absorber plate for both the flat plate and perforated plate with circular holes with a diameter of 3 mm over time. The figure shows that the flat plate's average temperature is higher than the perforated plate's. This is because the perforations allow air to flow through the plate, which increases heat exchange between the plate and the air, resulting in a lower average perforated plate temperature. This difference is important because using a perforated plate helps raise the solar collector's air temperature. At 13:00 PM, the average temperature of the perforated plate was about 8.5°C lower than that of the flat plate, which increased the collector outlet air temperature by

5.6°C. This increased air temperature enhances drying performance during peak solar hours and helps reduce energy consumption.
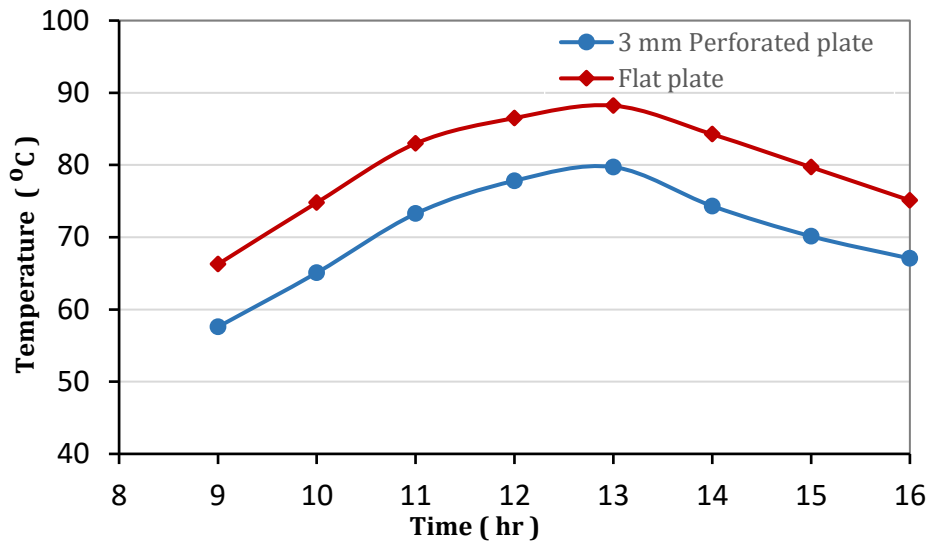
**Figure 7.** Average surface temperature for flat and perforated absorber plates over time.

The increase in air temperature denotes the quantity of thermal energy acquired when air passes the solar collector, representing the difference between the inlet and outlet temperatures of the collector. **Fig. 8a, 8b, and 8c** show an increase in the air temperature difference (ΔT) when using the perforated plate compared to the flat plate. This is attributed to the improved air and plate surface interaction heat transfer. The highest temperature difference occurred between 11:00 AM and 12:00 PM, coinciding with the increase in solar radiation intensity. At an air flow rate of 0.0113 m³/s, the difference was approximately 20.8°C for the perforated plate and 16.5°C for the flat plate. The figure also shows that increasing the air flow rate to 0.0226 m³/s decreased ΔT because the air contact time with the plate surface was reduced. These results support the system's effectiveness in hot and dry conditions for optimal drying.
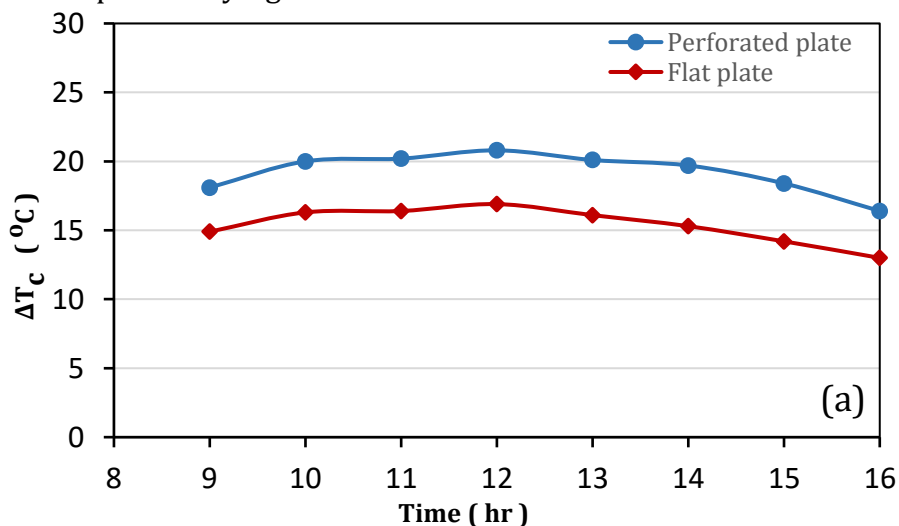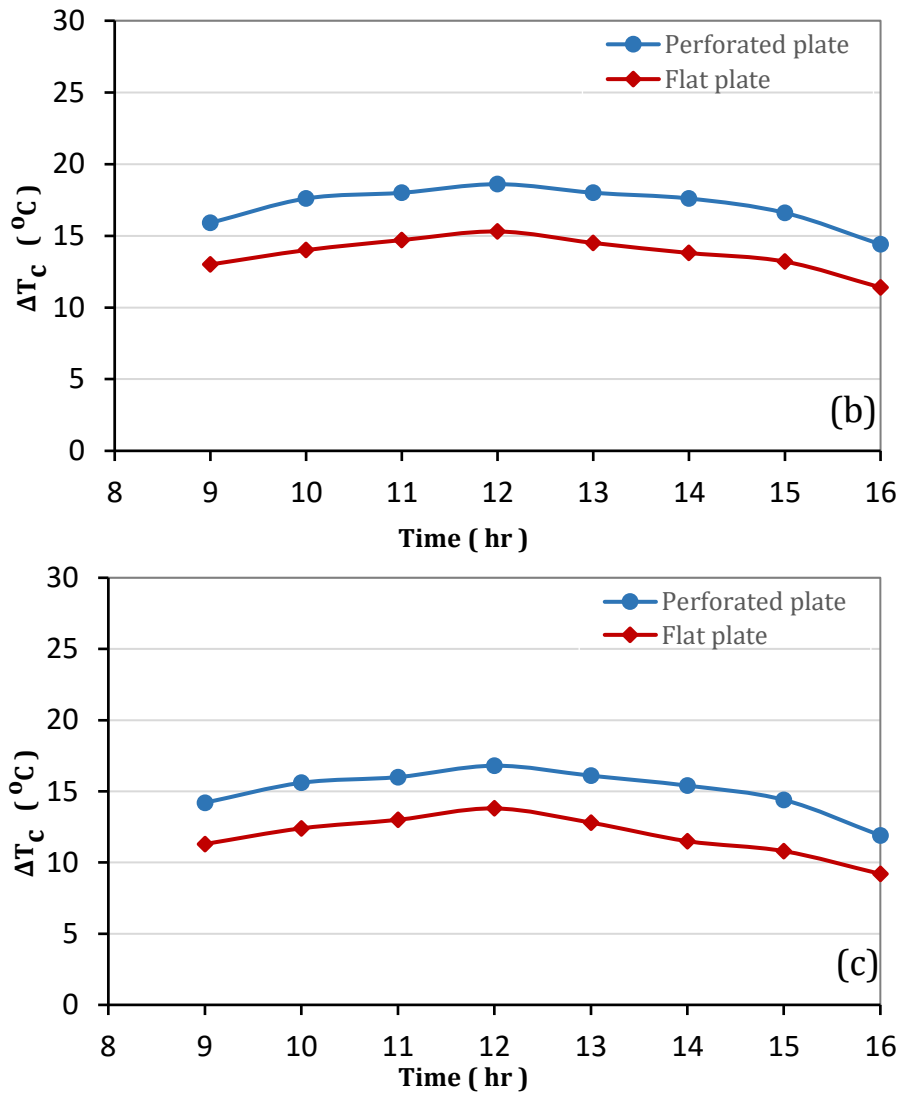
Figure 8. Variation in collector air temperature difference over time using flat and perforated absorber plates at airflow rates of (a) 0.0113 m³/s, (b) 0.0169 m³/s, and (c) 0.0226 m³/s.

Fig. 9a, 9b, and 9c show the effect of using a perforated and flat absorber plate at three airflow rates (0.0113, 0.0169, and 0.0226) m³/s on the performance of the collector thermal efficiency. The thermal efficiency of the collector depends on the air temperature difference (ΔT), airflow rate, and solar radiation. The figure demonstrates that the gain in the airflow rate improves the collector's thermal efficiency. The maximum values of the collector's thermal efficiency using the perforated and flat absorber plates are 49.8% and 44.2% at an airflow rate of 0.0113 m³/s, 66.12% and 57.5% at an airflow rate of 0.0169 m³/s, and 76% and 66.62% at an airflow rate of 0.0226 m³/s, respectively, at noon. These results demonstrate the system's effectiveness in capturing solar radiation and converting it into useful heat for heating the air, and this supports its practical use under hot conditions where efficient energy is essential for continuous agricultural drying.
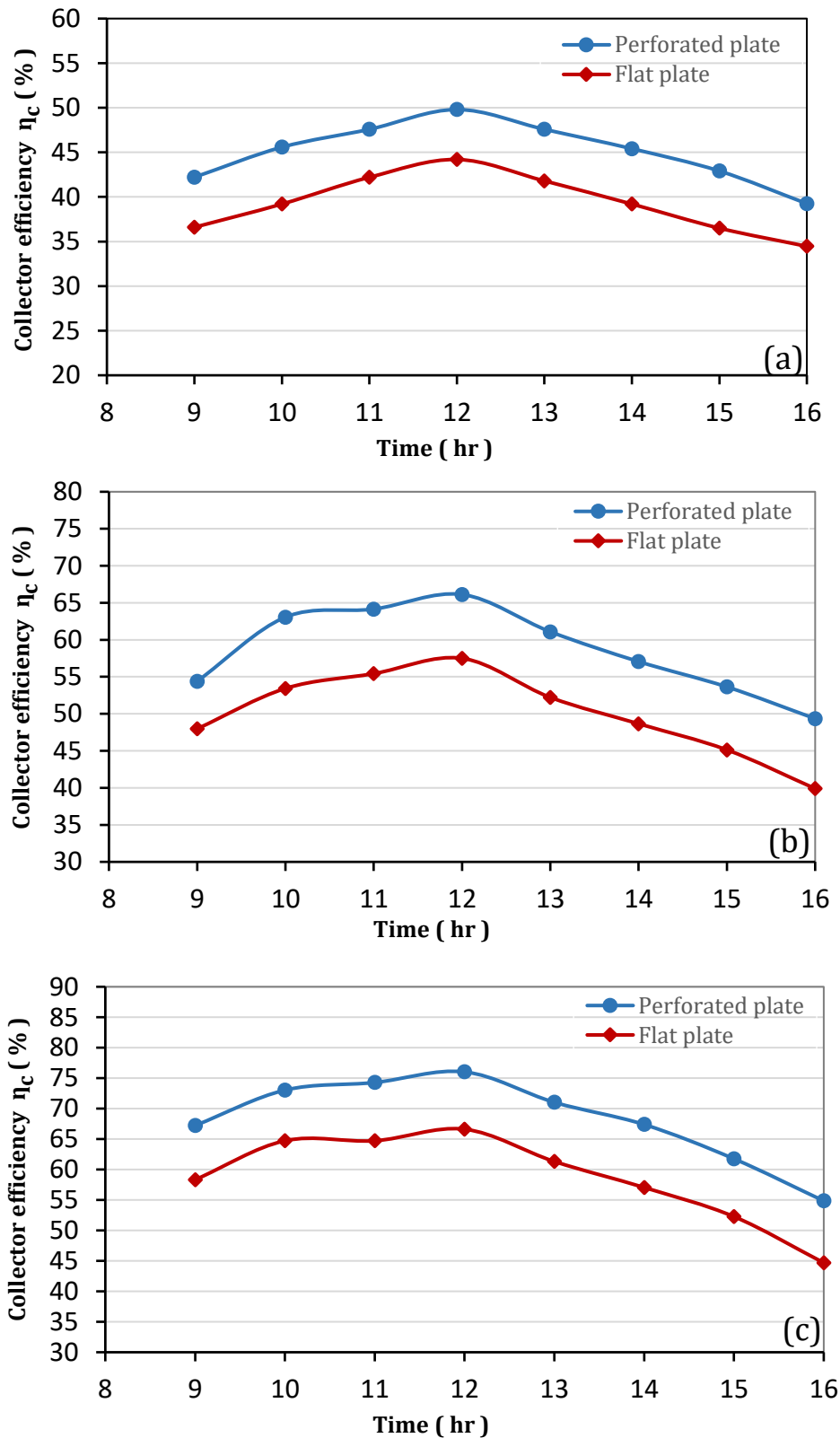
Figure 9. Variation in collector thermal efficiency over time using flat and perforated absorber plates at airflow rate; (a) 0.0113 m^3/s, (b) 0.0169 m^3/s, and (c) 0.0226 m^3/s.

The definition of dryer efficiency refers to the total effectiveness of a drying system **(Khidhir, 2023)**. Dryer efficiency for three airflow rates (0.0113, 0.0169, and 0.0226) m^3/s over time is illustrated in **Fig. 10a, 10b, and 10c**. From the figure, it can be noted that the maximum dryer efficiency was obtained at an airflow rate of 0.0113 m^3/s for the solar air collector with the perforated absorber plate and flat absorber plate, which are 28.44% and 22.22%, respectively, because the air temperature produced by the collector was higher at the airflow rate of 0.0113 m^3/s. It is noted that air temperature and velocity are important parameters for the drying process. Over time, the dryer efficiency gradually declined due to a reduction in the evaporation rate of the product moisture. These results demonstrate the practical importance of determining the appropriate airflow rate and absorber plate geometric design, which contributes to energy savings and improved dryer performance under hot climatic conditions in Iraq.

The drying rate indicates how quickly dehydration occurs in the dryer. **Fig. 11a, 11b, and 11c** show the change in the drying rate of the product over time for each hour of drying for three airflow rates (0.0113, 0.0169, and 0.0226) m^3/s. The curve trend falls in the earlier stages of the drying process, indicating significant evaporation in the product as air temperature rises.
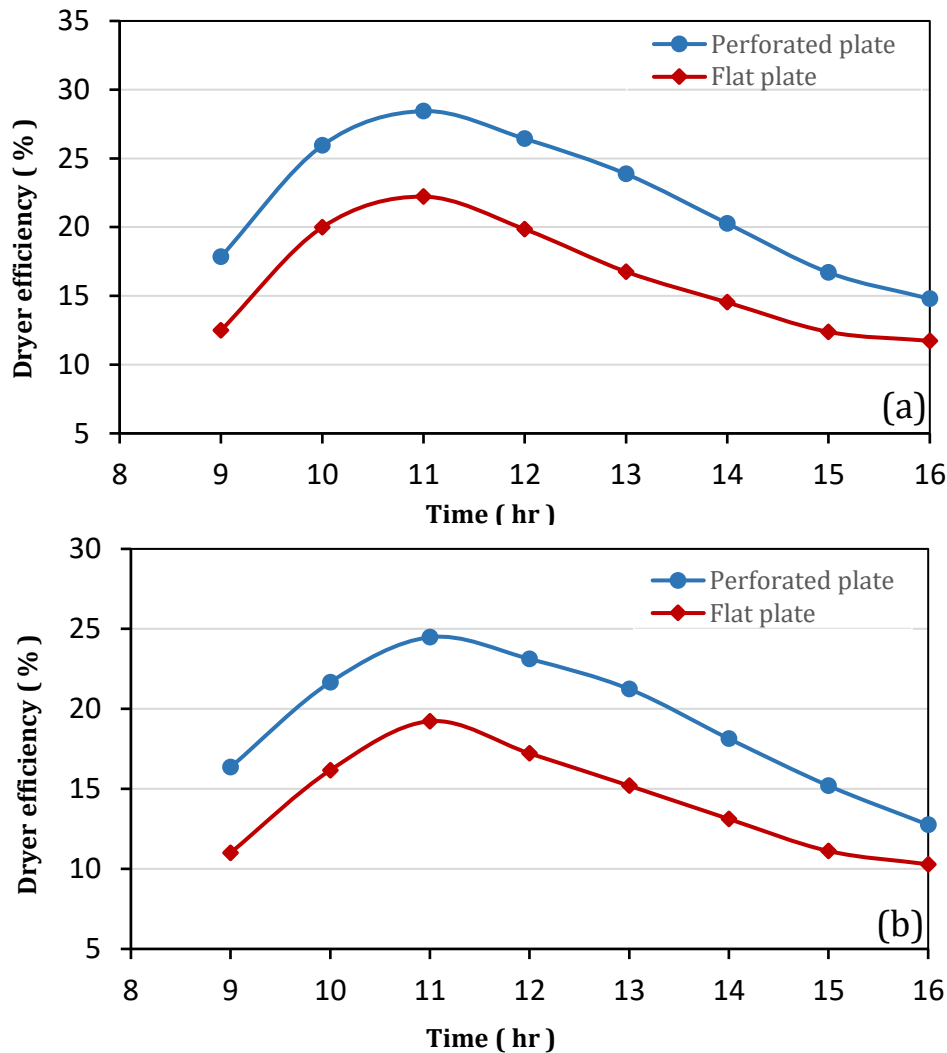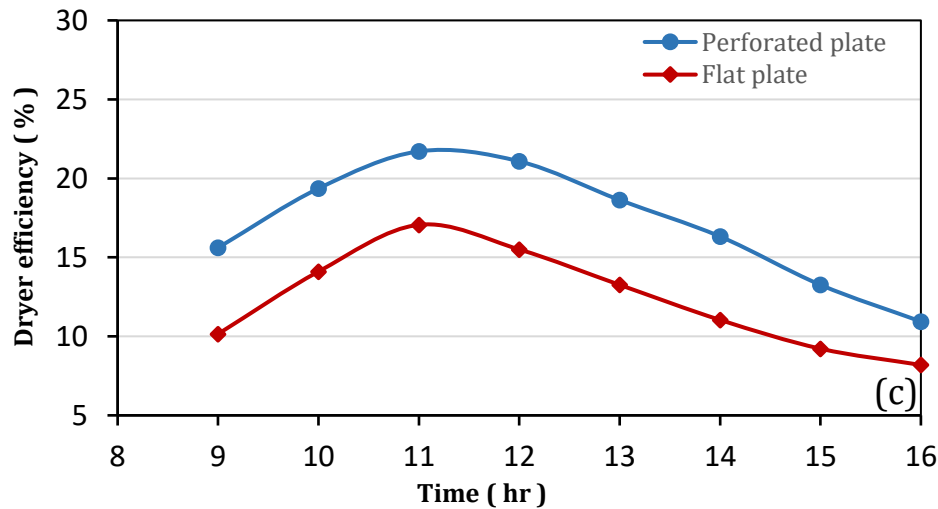
Figure 10. Variation of dryer efficiency with time at airflow rate; (a) 0.0113 m^3/s, (b) 0.0169 m^3/s, and (c) 0.0226 m^3/s.

The drying operation occurs in the falling rate period. During the falling rate period, the product surface is no longer saturated with water, allowing moisture diffusion from the product interior to the surface to determine the drying rate **(Akpinar, 2010)**. The figure shows that at an air flow rate of 0.0113 m^3/s, the maximum drying rate using the perforated plate was 0.68 kg/h, compared to 0.545 kg/h for the flat plate. The results show that fast drying helps reduce drying time, making the system more effective for practical use.
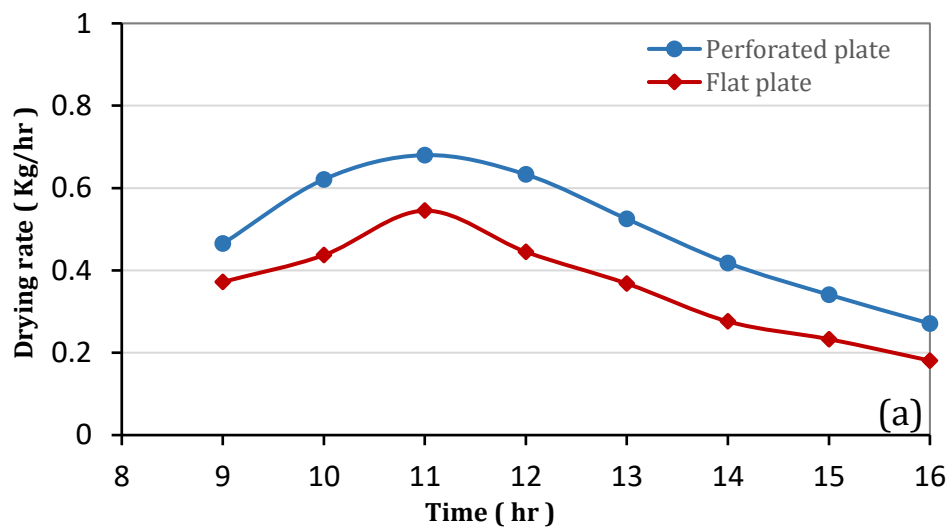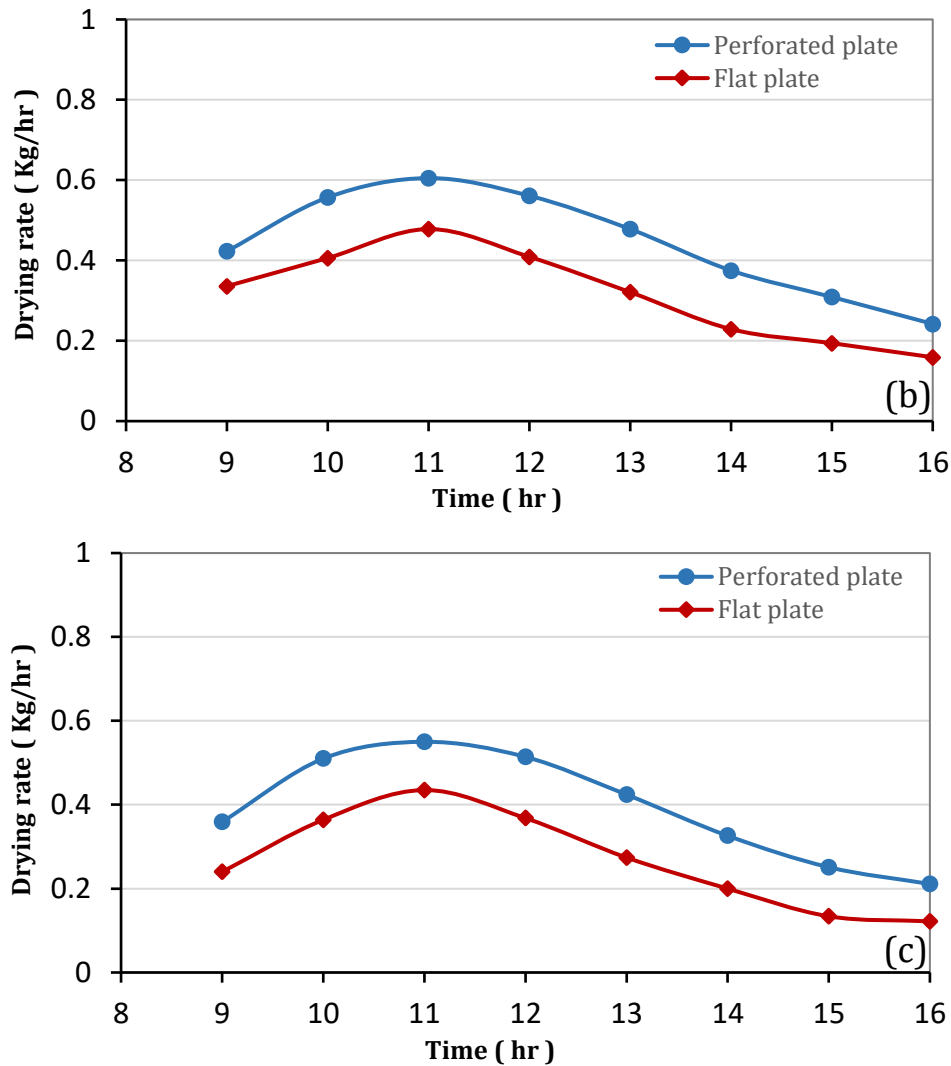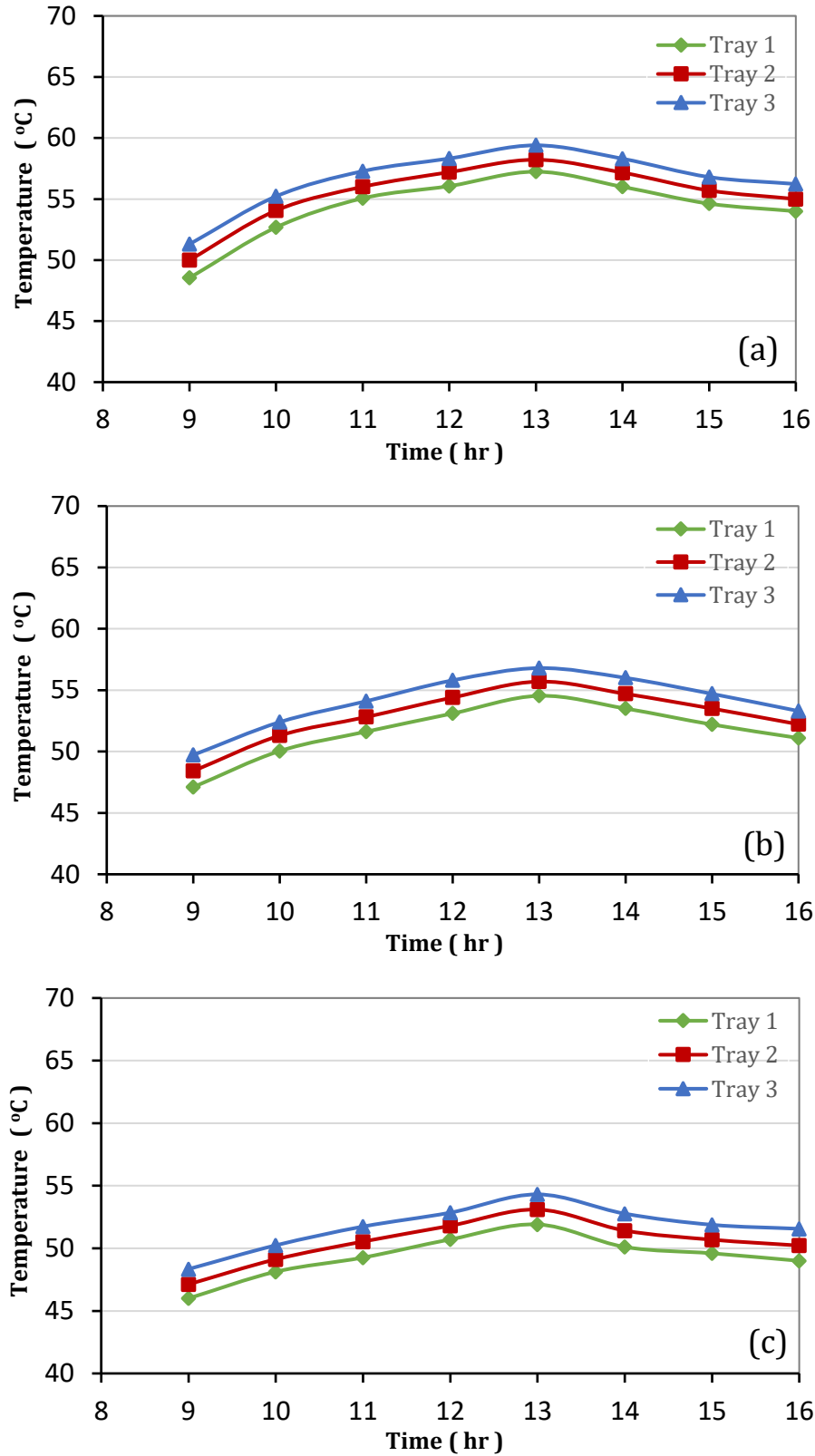
Figure 11. Variation of drying rate of apricots with the time at airflow rate; (a) 0.0113 m³/s, (b) 0.0169 m³/s, and (c) 0.0226 m³/s.

The variation of the average air temperature on the trays is shown in **Fig. 12a, 12b, and 12c**, and **Fig. 13a, 13b, and 13c** for three different airflow rates. There are no significant differences in temperature in the three trays. A vertical air distribution channel integrated into the drying chamber improves the drying process. The drying air temperature was distributed uniformly across the drying trays, which was observed. **Fig. 12** shows that the solar air collector with the perforated absorber plate at the airflow rate of 0.0113 m³/s is optimal for a more efficient drying process.
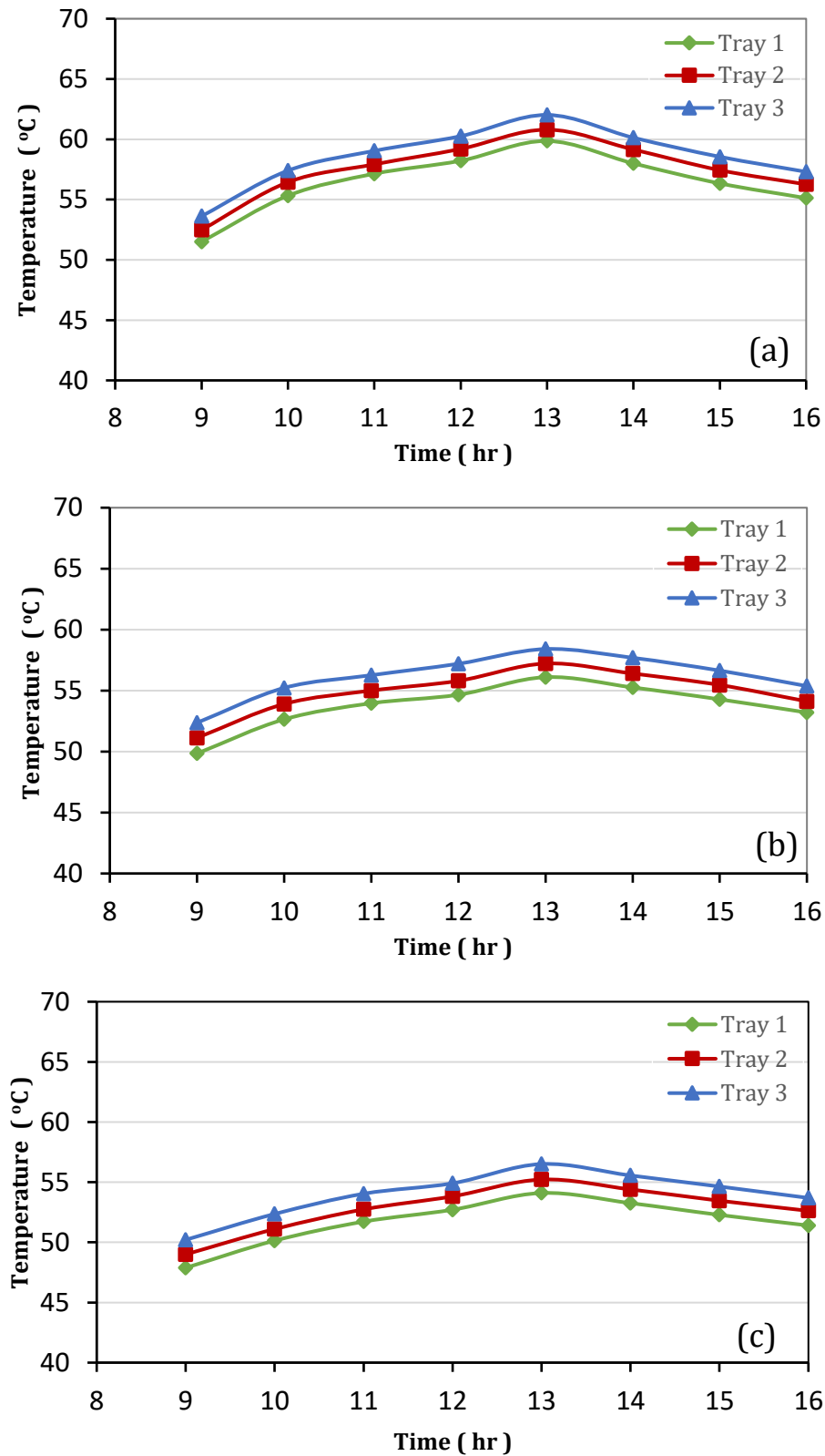
Figure 12. Variation of the average air temperature of each tray by using a perforated plate with circular holes (3 mm) with the time at airflow rate; (a) 0.0113 m³/s, (b) 0.0169 m³/s, and (c) 0.0226 m³/s.

Figure 13. Variation of the average air temperature of each tray by using a flat plate with the time at airflow rate; (a) 0.0113 m³/s, (b) 0.0169 m³/s, and (c) 0.0226 m³/s.

Fig. 14a, 14b, and 14c show the mass loss of the apricots for three airflow rates (0.0113, 0.0169, and 0.0226) m^3/s with time. The initial weight of apricots before drying was 3 kg in all cases. After the eight-hour duration of the drying procedure, the final weights when using the perforated plate were 1.700 kg, 1.738 kg, and 1.787 kg, while they were 1.798 kg, 1.836 kg, and 1.899 kg when using the flat plate for the same air flow rates, respectively. The decrease in mass is due to the moisture evaporation from the product. Thus, the product's water content decreases due to the temperature and airflow conditions within the drying chamber during the drying process. The results show that the highest apricot weight loss was approximately 1.300 kg using the perforated plate at the lowest airflow rate of 0.0113 m^3/s, which is optimal for a more efficient drying process. This means that using the solar dryer equipped with a perforated plate at a low airflow rate is optimal for practical applications in hot and dry environments, as it provides faster and more efficient drying, which reduces energy consumption, reduces drying time, and maintains the quality of the dried product.
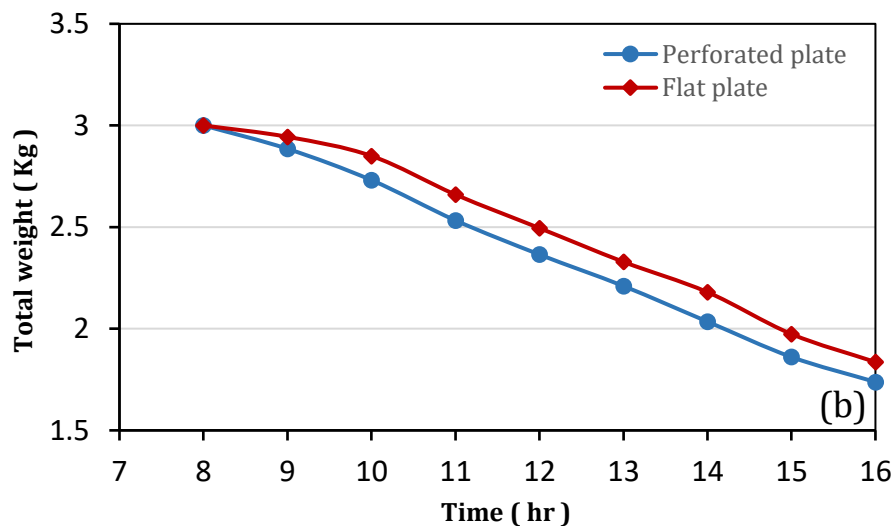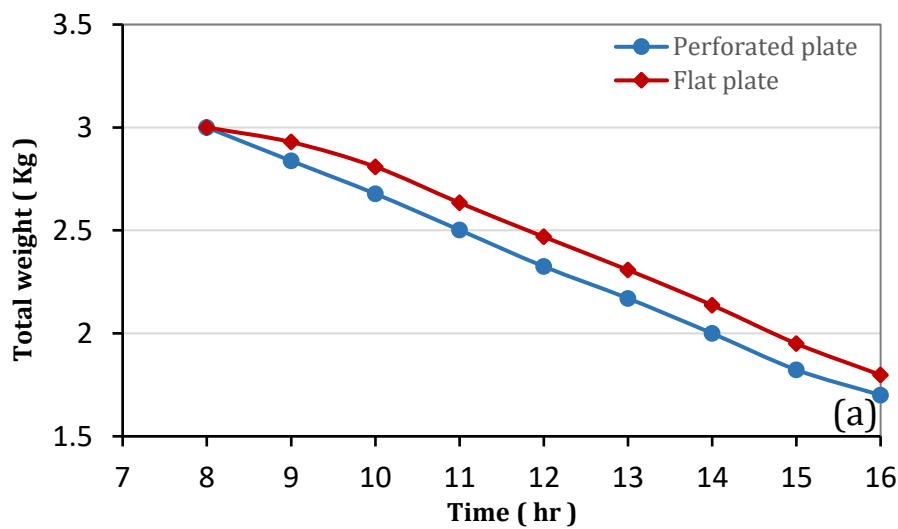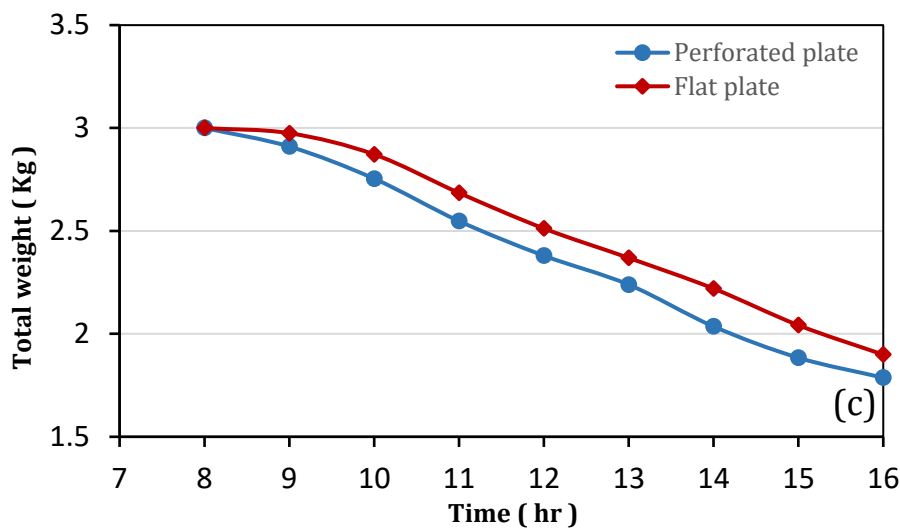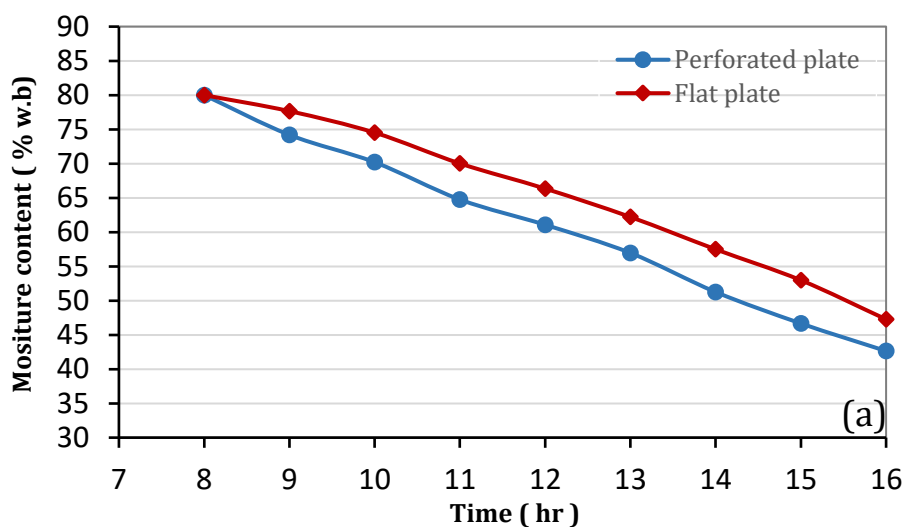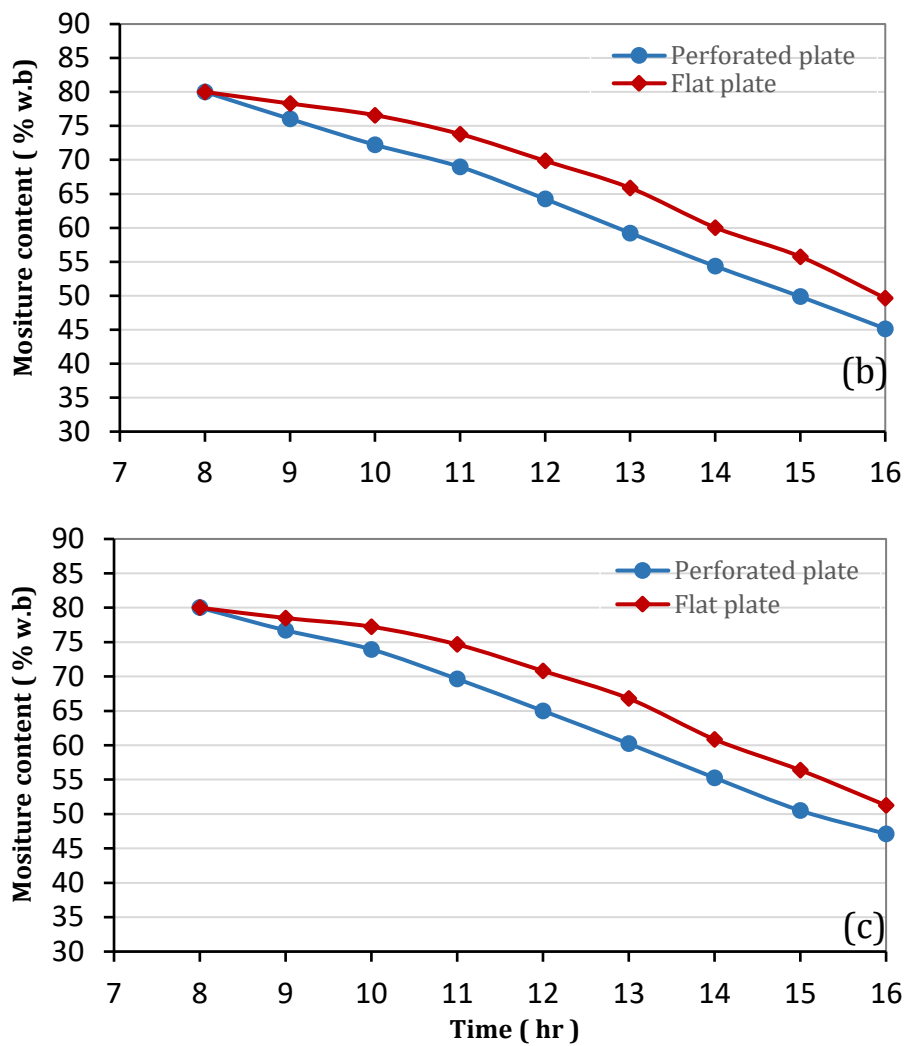
Figure 14. Variation of total weight of product with time at airflow rate; (a) 0.0113 m^3/s, (b) 0.0169 m^3/s, and (c) 0.0226 m^3/s.

Fig. 15a, 15b, and 15c show the variation of moisture content for three airflow rates (0.0113, 0.0169, and 0.0226) m^3/s with drying time. After operating the system for about 8 h, the moisture content decreases from 80% to 42%, 45%, and 47% when using the perforated plate, while it decreases to 47%, 49%, and 51% when using the flat plate for the same air flow rates, respectively. The results show the system's effectiveness in reducing product moisture content when using a perforated plate at a low airflow rate, which is essential for maintaining product quality, extending its storage period, and thus reducing post-harvest losses.

The variation of the air's relative humidity for three different airflow rates is presented in **Fig. 16a, 16b, and 16c**. In general, the air relative humidity is high in the beginning and then decreases as the moisture content of the product declines. This indicates that the evaporation rate declined as time passed.

Figure 15. Variation of moisture content of apricots with the time at airflow rate; (a) $0.0113 \text{ m}^3/\text{s}$, (b) $0.0169 \text{ m}^3/\text{s}$, and (c) $0.0226 \text{ m}^3/\text{s}$.
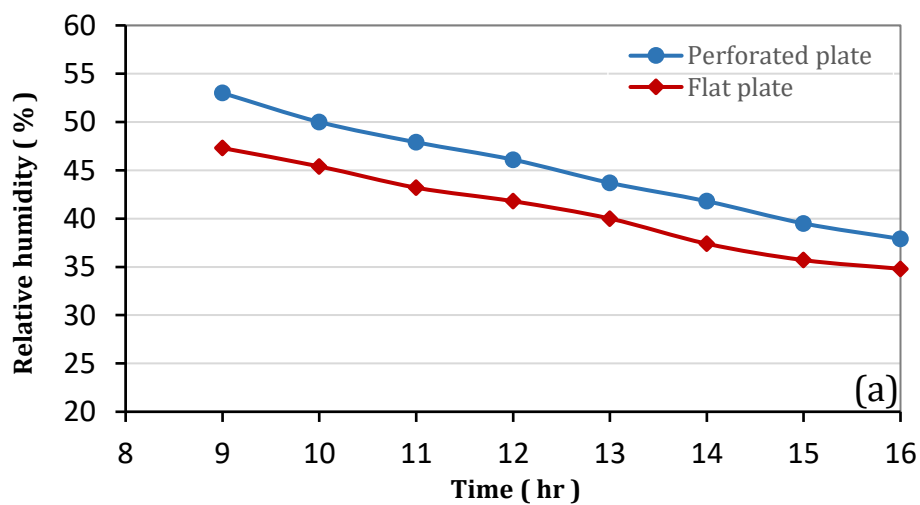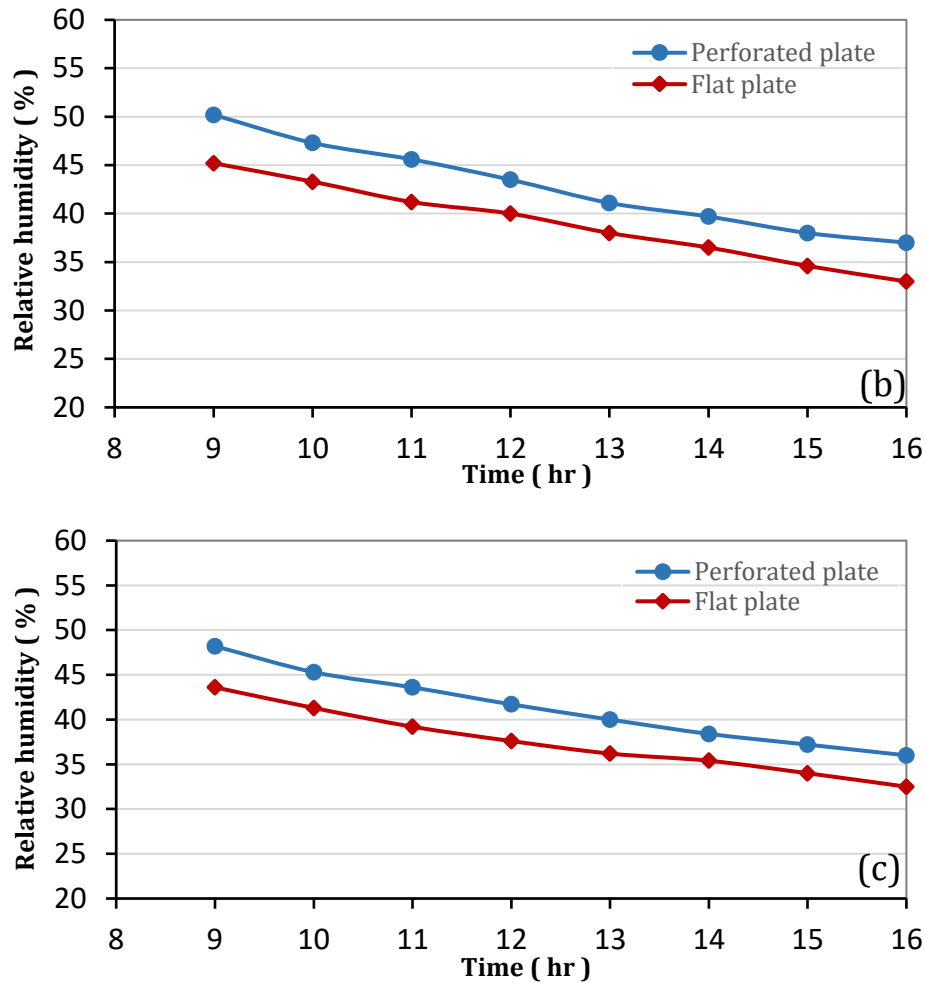
Figure 16. Variation of air relative humidity with time at airflow rate; (a) 0.0113 m^3/s, (b) 0.0169 m^3/s, and (c) 0.0226 m^3/s.

In the current study, the dryer effectively reduced the moisture content of apricots from 80% to 42% within 8 hours using a perforated absorption plate and a low airflow rate. This result demonstrates the efficiency of the drying process, which balances drying speed with product quality, which is critical for practical applications. In comparison **(Al-Juamily et al., 2007)** achieved a lower moisture content of 13%, but over a more extended drying period of about a day and a half, using a flat plate under the climatic conditions in Iraq, as shown in **Fig. 17**. While the system achieves deeper drying, longer drying times can increase energy consumption. Therefore, the solar dryer in the current study demonstrates a clear advantage in significantly reducing drying time while maintaining an acceptable moisture content for storage. This makes it suitable for practical applications in hot climates such as Iraq, where fast and efficient drying is critical to minimise post-harvest losses.
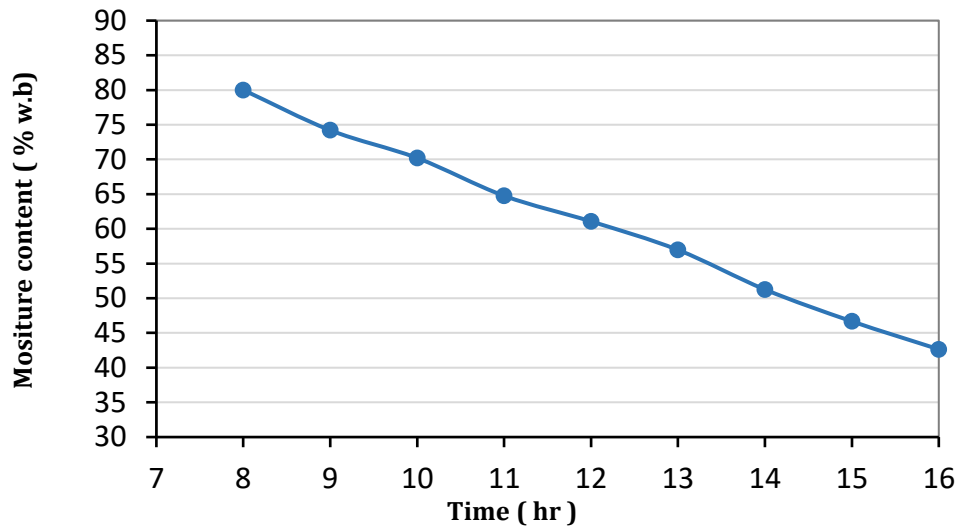
(a) Present work.
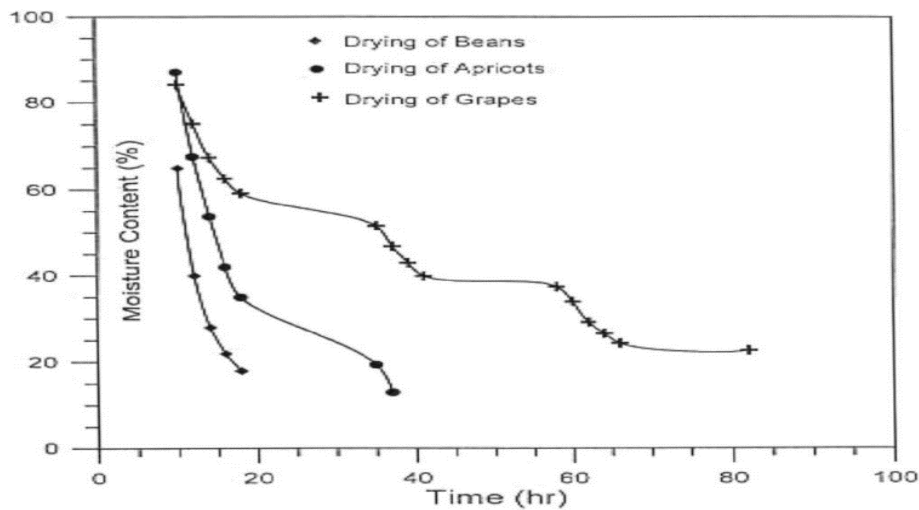
(b) **(Al-Juamily et al., 2007).**

Figure 17. Comparison of moisture content decrease over time.

5. CONCLUSIONS

The experimental work aimed to investigate the impact of varying the airflow rate on the performance of an indirect solar air dryer using the perforated plate with circular holes of diameter 3 mm, compared with a conventional flat absorber plate. The experimental research was conducted under Iraqi climate conditions. The solar intensity changed from 610 to 821.62 W/m². A concise summary of the key results from this study is provided below:

1. The results showed that the use of a perforated plate resulted in a significant improvement in thermal performance and overall dryer efficiency compared to a flat plate.
2. The average surface temperature of the perforated absorber plate decreases by about 9.63% compared to the flat plate, indicating improved heat exchange between the air and the perforated plate.

3. The highest collector air temperature difference (ΔT) was recorded when using the perforated absorption plate at a low airflow rate (0.0113 m^3/s), reaching 20.8°C, compared to 16.5°C for the flat plate.
4. The perforated absorber plate achieved the highest thermal efficiency of the solar collector, reaching 76% at 12:00 PM, compared to 66.62% for the flat plate, at the highest airflow rate (0.0226 m^3/s).
5. The drying performance was best at a low airflow rate (0.0113 m^3/s), where the apricot moisture content was reduced from 80% to 42% using the perforated plate, compared to 47% for the flat plate within 8 hours, with maximum drying efficiencies of 28.44% and 22.22%, respectively.

NOMENCLATURE

Symbol	Description	Symbol	Description
A_{duct}	Area of the airflow duct (m²)	MC	Moisture content (%)
Ac	Area of the solar collector (m²)	M_I	Initial moisture content (%)
C_p	Specific heat (J/Kg °C)	M_F	Final moisture content (%)
d_{duct}	Dimeter of the duct (m)	m_w	The evaporated water mass (Kg)
h_{fg}	The latent heat vaporization for water (KJ/Kg)	m_{dr}	The drying rate (Kg/hr)
I	Total value of incident solar radiation intensity (W/m²)	Q_{solar}	The input thermal solar radiation (W)
$\dot{m}$	Air mass flow rate (Kg/s)	Q_u	The useful heat energy (W)
m_i	Mass of the sample before drying (Kg)	T_i	The temperature of the solar air collector inlet (°C)
m_f	Mass of the sample after drying (Kg)	T_o	The temperature of the solar air collector outlet (°C)

Acknowledgements

Credit Authorship Contribution Statement

Ghadeer Qasim Fadhil: Writing – review & editing, Writing – original draft, Validation, Software, Methodology. Sarmad A. Abdul Hussein: Supervising and following up the research.

Declaration of Competing Interest

The authors declare that they have no known competing financial interests or personal relationships that could have appeared to influence the work reported in this paper.

REFERENCES

Akpinar, E.K., 2010. Drying of mint leaves in a solar dryer and under open sun: Modelling, performance analyses. *Energy Conversion and Management*, 51(12), pp. 2407-2418. https://doi.org/10.1016/j.enconman.2010.05.005.

Al-Juamily, K.E.J., Khalifa, A.J.N., and Yassen, T.A., 2007. Testing of the performance of a fruit and vegetable solar drying system in Iraq. *Desalination*, 209(1-3), pp. 163-170. https://doi.org/10.1016/j.desal.2007.04.026.

Al-Neama, M.A.J., 2018. Performance enhancement of solar air collectors applied for drying processes. PhD. Thesis, Faculty of Mechanical Engineering, Szent Stván University, Gödöllő, Hungary.

Arunkumar, P.M., Balaji, N., and Madhankumar S., 2024. Performance analysis of indirect solar dryer with natural heat energy retention substances for drying red chilli. *Sustainable Energy Technologies and Assessments*, 64, P. 103706. https://doi.org/10.1016/j.seta.2024.103706.

Babar, O.A., Tarafdar, A., Malakar, S., Arora, V.K., and Nema, P.K., 2020. Design and performance evaluation of a passive flat plate collector solar dryer for agricultural products. *Journal of Food Process Engineering*. http://dx.doi.org/10.1111/jfpe.13484.

Bhavsar, H.P., and Patel, C.M. 2021. Performance investigation of natural and forced convection cabinet solar dryer for ginger drying. *In Materials Today: Proceedings, 47(Part 17), pp. 6128-6133.* https://doi.org/10.1016/j.matpr.2021.05.050.

El-Sebaey, M.S., 2024. Proposing novel approach for indirect solar dryer integrated with active-fan and passive-chimney: An experimental and analytical investigation. *Energy*, 304, P. 132215. https://doi.org/10.1016/j.energy.2024.132215.

Ennissioui, J., Benghoulam, E.l. M., and El Rhafiki, T., 2023. Experimental study of a natural convection indirect solar dryer. *Heliyon*, 9(11), pp. e21299. https://doi.org/10.1016/j.heliyon.2023.e21299.

Essalhi, H., Tadili, R., and Bargach, M.N., 2017. Conception of a solar air collector for an indirect solar dryer. pear drying test. *Energy Procedia*, 141, pp. 29-33. https://doi.org/10.1016/j.egypro.2017.11.114.

Farhan, A.A., and Sahi, H.A., 2017. Energy analysis of solarc with perforated absorber plate*. Journal of Engineering*, 23(9), pp. 89-102. https://doi.org/10.31026/j.eng.2017.09.07.

Fernandes, L., Fernandes, J.R., and Tavares, P.B., 2022. Design of a friendly solar food dryer for domestic over-production. *Solar*, 2(4), pp. 495–508. http://dx.doi.org/10.3390/solar2040029.

Gilago, M.C., and Chandramohan, V.P., 2022. Performance evaluation of natural and forced convection indirect type solar dryers during drying ivy gourd: An experimental study. *Renewable Energy*, 182, pp. 934-945. https://doi.org/10.1016/j.renene.2021.11.038.

Hegde, V.N., Hosur, V.S., Rathod, S.K., Harsoor, P.A., and Narayana, K.B., 2015. Design, fabrication and performance evaluation of solar dryer for banana. *Energy, Sustainability and Society*, 5(1), pp. 1-12. http://dx.doi.org/10.1186/s13705-015-0052-x.

Jadallah, A.A., Alsaadi, M.K., and Hussien, S.A., 2020. The hybrid (PVT) double-pass system with a mixed-mode solar dryer for drying banana. *Engineering and Technology Journal*, 38(08), pp. 1214-1225. https://doi.org/10.30684/etj.v38i8A.535.

Jassim, N.A., and Shbailat, S.J., 2018. Energy and exergy analysis of dual channel solar air collector with different absorber plates geometry. *Journal of Engineering*, 24(4), pp. 19-40. https://doi.org/10.31026/j.eng.2018.04.02.

Khan, Y., Kasi, J.K., and Kasi, A.K., 2018. Dehydration of vegetables by using indirect solar dryer. *Scientific Journal of Mehmet Akif Ersoy University*, 1(1), pp. 22-28.

Khidhir, D.K., 2023. Manufacturing and evaluating of indirect solar dryers: A case study for the kurdistan region of Iraq. *Aro-The Scientific Journal of Koya University*, 11(2), pp. 89-94. http://dx.doi.org/10.14500/aro.11127.

Kilanko, O., Ilori, T.A., Leramo, R.O., Babalola, P.O., Eluwa, S.E., Onyenma, F.A., Ameh, N.I., Onwordi, P.N., Aworinde, A.K., and Fajobi, M.A., 2019. Design and Performance Evaluation of a Solar Dryer. *Journal of Physics: Conference Series*, 1378(3), P. 032001. http://dx.doi.org/10.1088/1742-6596/1378/3/032001.

Kokate, Y.D., Baviskar, P.R., Baviskar, K.P., Deshmukh, P.S., Chaudhari, Y.R., and Amrutkar, K.P., 2023. Design, fabrication and performance analysis of indirect solar dryer. *Materials Today: Proceedings*, 77(Part 3), pp. 748-753. https://doi.org/10.1016/j.matpr.2022.11.439.

Krabch, H., Tadili, R., Idrissi, A., and Bargach, M., 2022. Indirect solar dryer with a single compartment for food drying. Application to the drying of the pear. *Solar Energy*, 240(1), pp. 131-139. https://doi.org/10.1016/j.solener.2022.05.025.

Kumar, A., Singh, K.U., Singh, M.K., Kushwaha, A.K.S., Kumar, A., and Mahato, S., 2022. Design and fabrication of solar dryer system for food preservation of vegetables or fruit. *Journal of Food Quality*,(1), pp. 1-14. http://dx.doi.org/10.1155/2022/6564933.

Lingayat, A.B., Chandramohan, V.P., Raju, V.R.K., and Meda, V., 2020. A review on indirect type solar dryers for agricultural crops – Dryer setup, its performance, energy storage and important highlights. *Applied Energy*, 258, P. 114005. https://doi.org/10.1016/j.apenergy.2019.114005.

Mugi, V.R., Gilago, M.C., and Chandramohan, V.P., 2022. Energy and exergy investigation of indirect solar dryer under natural and forced convection while drying muskmelon slices. Energy Nexus, 8, P. 100153. https://doi.org/10.1016/j.nexus.2022.100153.

Nabnean, S., and Nimnuan, P., 2020. Experimental performance of direct forced convection household solar dryer for drying banana. *Case Studies in Thermal Engineering*, 22, P. 100787. https://doi.org/10.1016/j.csite.2020.100787.

Natarajan, S.K., Suraparaju, S.K., Muthuvairavan, G., Elangovan, E., and Samykano, M., 2024. Experimental analysis and development of novel drying kinetics model for drying grapes in a double slope solar dryer. *Renewable Energy*, 236, P. 121508. https://doi.org/10.1016/j.renene.2024.121508.

Ndukwu, M.C., Ibeh, M., Okon, B.B., Akpan, G., Kalu, C.A., Ekop, I., Nwachukwu, C.C., Abam, F.I., Lamrani, B.,Tagne, M.S., Ben, A.E., Mbanasor, J., and Bennamoun, L., 2023. Progressive review of solar drying studies of agricultural products with exergoeconomics and econo-market participation aspect. *Cleaner Environmental Systems*, 9, P. 100120. https://doi.org/10.1016/j.cesys.2023.100120.

Nhut, L.M., Hien, H.T.T., and Lam, N.X., 2020. Development of solar air collector with crimped baffles for drying applications. *International Journal of Engineering Research*, 9(03). http://dx.doi.org/10.17577/IJERTV9IS030156.

Rezaei, M.H., Sefid, M., Almutairi, K., Mostafaeipour, A., Ao, H.X., Dehshiri, S.J.H., Dehshiri, S.S.H., Chowdhury, S., and Techato, K., 2022. Investigating performance of a new design of forced convection solar dryer. *Sustainable Energy Technologies and Assessments*, 50, P. 101863. https://doi.org/10.1016/j.seta.2021.101863.

Salhi, M., Chaatouf, D., Bria, A., Amraqui, S., and Mezrhab, A., 2024. Experimental assessment of a new prototype solar dryer integrated with a photovoltaic system. *Energy for Sustainable Development*, 81, P. 101518. https://doi.org/10.1016/j.esd.2024.101518.

Sileshi, S.T., Hassen, A.A., and Adem, K.D., 2022., Simulation of mixed-mode solar dryer with vertical air distribution channel. *Heliyon*, 8(11), P. e11898. https://doi.org/10.1016/j.heliyon.2022.e11898.

Srithanyakorn, S., Bunchan, S., Krittacom, B., and Luampon, R., 2023. Comparison of mixed-mode forced-convection solar dryer with and without stainless wire mesh in solar collector. *Clean Energy*, 7(6), pp. 1316–1329. https://doi.org/10.1093/ce/zkad058.

Ssemwanga, M., Makule, E., and Kayondo, S.I., 2020. Performance analysis of an improved solar dryer integrated with multiple metallic solar concentrators for drying fruits. *Solar Energy*, 204(1), pp. 419-428. https://doi.org/10.1016/j.solener.2020.04.065.

Tagne, M.S., Etala, H.D.T., Tagne, A.T., Ndukwu, M.C., and El Marouani, M., 2022. Energy, environmental and economic analyses of an indirect cocoa bean solar dryer: A comparison between natural and forced convections. *Renewable Energy*, 187, pp. 1154-1172. https://doi.org/10.1016/j.renene.2022.02.015.

Vijayan, S., Arjunan, T.V., and Kumar, A., 2020. Exergo-environmental analysis of an indirect forced convection solar dryer for drying bitter gourd slices. *Renewable Energy*, 146, pp. 2210-2223. https://doi.org/10.1016/j.renene.2019.08.066.

Zeeshan, M., Tufail, I., Khan, S., Khan, I., Ayuob, S., Mohamed, A., and Chauhdary, S.T., 2024. Novel design and performance evaluation of an indirectly forced convection desiccant integrated solar dryer for drying tomatoes in Pakistan. *Heliyon*, 10(8), P. e29284. https://doi.org/10.1016/j.heliyon.2024.e29284.

تأثير تغير معدل تدفق الهواء على أداء مجفف شمسي غير مباشر باستخدام ألواح امتصاص مسطحة ومثقبة

غدير قاسم فاضل *، سرمد عزيز عبد الحسين

قسم الهندسة الميكانيكية، كلية الهندسة، جامعة بغداد، العراق، بغداد

الخلاصة

أُجري تحليل تجريبي لدراسة تأثير تغيير معدل تدفق الهواء الداخل إلى حجرة التجفيف على أداء مجفف شمسي غير مباشر يعمل بنظام الحمل القسري، وذلك في ظل الظروف المناخية لمدينة بغداد، العراق، عند خط عرض 33.3° شمالًا. تم اختبار أداء المجفف عند ثلاثة معدلات تدفق هواء (0.0113، 0.0169، و0.0226) م^3/ث ، باستخدام صفيحة امتصاص مسطحة تقليدية وأخرى مثقبة تحتوي على فتحات دائرية بقطر 3 مم. جُفّف المشمش في جميع التجارب التي أُجريت خلال شهر يونيو 2024. أظهرت النتائج أن الصفيحة المثقبة عززت الكفاءة الحرارية للمجمع الشمسي بشكل ملحوظ مقارنة بالصفيحة المسطحة، إذ حسّنت التبادل الحراري من خلال إحداث اضطراب في طبقة الحدود الحرارية وتحسين تدفق الهواء. كما أشارت النتائج إلى أن معدل تدفق الهواء المنخفض (0.0113 م^3/ث) حقق أفضل كفاءة تجفيف، حيث خُفِّض محتوى رطوبة المشمش من 80% إلى 42% باستخدام الصفيحة المثقبة، و47% باستخدام الصفيحة المسطحة خلال 8 ساعات، مع تسجيل أقصى كفاءة تجفيف بلغت 28.44% و22.22% على التوالي. وعلى الرغم من أن معدل تدفق الهواء الأعلى (0.0226 م^3/ث) قد حسّن الكفاءة الحرارية للمجمع، إلا أنه كان أقل فعالية في تحسين عملية التجفيف. أظهرت نتائج هذه الدراسة أن تشغيل مجفف شمسي غير مباشر باستخدام صفيحة ماصة مثقبة بمعدل تدفق هواء منخفض يسرّع من إزالة الرطوبة من المنتج مع الحفاظ على جودته، مما يجعل النظام مناسبًا للتطبيقات الزراعية العملية في البيئات الحارة والجافة، حيث تُعد سرعة وكفاءة التجفيف أمرًا بالغ الأهمية لتقليل خسائر ما بعد الحصاد وزيادة مدة تخزين المنتج.

الكلمات المفتاحية: معدل تدفق الهواء، الكفاءة الحرارية للمجمع، كفاءة المجفف، الحمل الحراري القسري، مجفف الهواء الشمسي غير المباشر.